Low-Temperature Electron Transfer in Photosystem II: A Tyrosyl Radical and Semiquinone Charge Pair†

Chunxi Zhang,‡ Alain Boussac, and A. William Rutherford*

Service de Bioénergétique, CNRS URA 2096, Département de Biologie Joliot-Curie, CEA Saclay, 91191 Gif-sur-Yvette, Cedex, France

Received June 30, 2004; Revised Manuscript Received August 20, 2004

ABSTRACT: The states induced by illumination at 7 K in the oxygen-evolving enzyme (PSII) from *Thermosynechococcus elongatus* were studied by EPR. In the S_0 and S_1 redox states, two $g \approx 2$ EPR signals, a split signal and a $g = 2.03$ signal, respectively, were generated by illumination with visible light. These signals were comparable to those already reported in plant PSII in terms of their g value, shape, and stability at low temperatures. We report that the formation and decay of these signals correlate with EPR signals from the semiquinone of the first quinone electron acceptor, Q_A^-. The light-induced EPR signals from oxidized side-path electron donors (Cyt b_{559}, Car, and Chl_Z) were also measured, and from these and the signals from Q_A^-, estimates were made of the proportion of centers involved in the formation of the $g \approx 2$ signals (approximately 50% in S_0 and 40% in S_1). Comparisons with the signals generated in plant PSII indicated approximately similar yields for the S_0 split signal. A single laser flash at 7 K induced more than 75% of the maximum split and $g = 2.03$ EPR signal observed by continuous illumination, with no detectable oxidation of side-path donors. The matching electron acceptor side reactions, the high quantum yield, and the relatively large proportion of centers involved support earlier suggestions that the state being monitored is $Tyr_Z^{\bullet}Q_A^-$, with the $g \approx 2$ EPR signals arising from $Tyr_Z^{\bullet}$ interacting magnetically with the Mn complex. The current picture of the photochemical reactions occurring in PSII at low temperatures is reassessed.

Photosystem II (PSII)[1] is a membrane-bound pigment−protein complex that catalyzes the oxidation of water to oxygen and the reduction of plastoquinone to plastoquinol by using light energy. The structure of cyanobacterial PSII was recently reported by three groups at 3.8−3.5 Å resolution (*1*−*3*), with the most recent report being a refined structure (*3*). Upon excitation, the primary electron donor, a chlorophyll species (P_{680}) in the reaction center, donates one electron to the primary electron acceptor (Pheo), producing $P_{680}^{+\bullet}$ and $Pheo^{-\bullet}$. The $Pheo^{-\bullet}$ then delivers an electron to Q_A^-, which then transfers that electron to Q_B. $P_{680}^{+\bullet}$ oxidizes D1-Tyr161, Tyr_Z, and the Tyr_Z radical oxidizes the Mn cluster. The Mn cluster is the catalytic site for water oxidation, which is made up of four Mn ions and one Ca^{2+}. The turnover of the Mn cluster involves five different states (S_n, $n = 0-4$), in which the S_0 state is the most reduced state and the S_1 state is the dark stable state (see refs *4*−*8* for reviews).

Tyr_Z is located between P_{680} and the Mn cluster and links the one-electron photochemical reaction and the four-electron catalytic water oxidation process (*4*−*8*). In active PSII, Tyr_Z donates an electron to $P_{680}^{+\bullet}$ mainly on a time scale ranging from tens of nanoseconds to a few hundreds of nanoseconds, forming a Tyr_Z radical. The reduction of $Tyr_Z^{\bullet}$ by an electron from the Mn cluster and the substrate water occurs in the tens of microseconds to millisecond time scale. One key issue is understanding the role of the Tyr_Z radical in active PSII. Despite its importance, spectroscopic studies of the Tyr_Z have been limited. This is partially because of the short lifetime of the Tyr_Z radical in the intact system. Trapping of the Tyr_Z radical has been carried out in inhibited PSII samples [e.g., Mn depletion (*9*−*11*), Ca depletion (*12*, *13*), etc.] by illumination at temperatures between 25 and −25 °C followed by rapid cooling. The properties of the Tyr_Z radical in these inhibited samples are thought to be quite different from those in the intact enzyme (*14*, *15*).

Charge separation takes place at low temperatures, forming $P_{680}^{+\bullet}Q_A^-$ in high yield, and this recombines in few milliseconds (*16*). It had been thought that Tyr oxidation would not occur at low temperatures since its oxidation is expected to require the loss of the phenolic proton (*17*) and most of the work in the literature on the low-temperature photochemistry seemed to uphold that view (*18*−*21*). This view has recently changed.

It was demonstrated that the redox active D2-Tyr160, Tyr_D, can undergo oxidation at temperatures as low as 1.8 K at high pH ($pK_a = 7.5$) in Mn-depleted PSII (*22*, *23*). While no such oxidation was observed for Tyr_Z at any pH tested

† This work was supported by a training grant to C.Z. from the DRI of the CEA.

* To whom correspondence should be addressed. E-mail: Rutherford@dsvidf.cea.fr. Fax: +33-1-69088717.

‡ Present address: Institute of Chemistry, Chinese Academy of Sciences, Beijing 100080, China.

[1] Abbreviations: Car, β-carotene; Chl, chlorophyll; Chl_Z, chlorophyll$_Z$; Cyt b_{559}, cytochrome b_{559}; Cyt c_{550}, cytochrome c_{550}; EPR, electron paramagnetic resonance; EDTA, ethylenediaminetetraacetic acid; MES, 4-morpholineethanesulfonic acid; P_{680}, primary electron donor of PSII; Pheo, pheophytin; PPBQ, phenyl-*p*-benzoquinone; PSII, photosystem II; Q_A and Q_B, primary and secondary quinone electron acceptors, respectively; Tyr_D, tyrosine 160 of the D_2 protein; Tyr_Z, tyrosine 161 of the D_1 protein.

10.1021/bi048631j CCC: $27.50
Published on Web 10/05/2004

in Mn-depleted PSII (*22*), this did raise the possibility that in the intact enzyme this might occur. This is particularly relevant because phenomena attributed to $Tyr_Z^{\bullet}$ formation in intact PSII have been reported (*24*−*28*). Two metalloradical $g \approx 2$ EPR signals, a split signal in the S_0 state (*25*) and a $g = 2.03$ signal in S_1 (*24*−*26*), were formed in active PSII when it was illuminated with visible light at liquid helium temperature (see also refs *27* and *28*). By analogy to the better-studied $S_2Tyr_Z^{\bullet}$ "split signals" generated from inhibited PSII [e.g., Ca depletion (*12*, *13*)] and from a range of circumstantial evidence, it was proposed that these low-temperature signals arise from $Tyr_Z^{\bullet}$ interacting with the Mn cluster in the S_1 and S_0 states (*24*−*28*). While this attribution is reasonable, firm evidence is lacking.

In this paper, we have attempted to clarify the origins of these "metalloradical" EPR signals. First we have looked for their presence in highly active cyanobacterial PSII. Second, we have attempted to correlate the formation of the "split" signals with the corresponding reduced electron acceptor, Q_A^-, which is assumed in all the reports but up to now remained poorly defined. Third, we have attempted to quantify the number of centers that undergo this reaction, something that has been attempted in previous articles but which has yet to provide an unambiguous answer. At the same time, we have monitored and quantified the photochemistry occurring in centers where the metalloradical signal is not formed. Last, we have measured the yield of formation of the charge pair formed by a single laser flash at low temperatures.

MATERIALS AND METHODS

PSII-enriched membranes from spinach were prepared as described in refs *29* and *30*. The PSII membranes were suspended in a medium containing 400 mM sucrose, 15 mM NaCl, and 50 mM MES/NaOH (pH 6.0) (5 mg/mL Chl), frozen in liquid nitrogen, and stored at −80 °C until they were used. The PSII core complex from *Thermosynechococcus elongatus* was prepared as described in ref *31* and stored at −80 °C in a medium containing 10% glycerol, 15 mM $CaCl_2$, 15 mM $MgCl_2$, and 40 mM MES/NaOH (pH 6.5, 1 mg of Chl/mL).

To prepare EPR samples, samples of the plant PSII membrane were thawed on ice, then washed once with 400 mM sucrose, 15 mM NaCl, 5 mM $CaCl_2$, 5 mM $MgCl_2$, 2 mM EDTA, 25 mM MES/NaOH (pH 6.5) buffer, and then washed with a similar buffer without EDTA. Finally, the samples were suspended in 400 mM sucrose, 15 mM NaCl, 5 mM $CaCl_2$, 5 mM $MgCl_2$, 25 mM MES/NaOH (pH 6.5), and 1.3 M betaine. PSII membranes with the Mn cluster in different S states were prepared by using laser flashes at room temperature as described in refs *25* and *32* in the presence of 0.5 mM PPBQ.

For PSII core complexes from *T. elongatus*, samples were thawed on ice and then washed twice to remove the glycerol with buffer containing 400 mM sucrose, 15 mM NaCl, 5 mM $CaCl_2$, 5 mM $MgCl_2$, 1.3 M betaine, and 25 mM MES/NaOH (pH 6.5). Washing was done by centrifugation at 50000*g* for 24 h to pellet the PSII complexes, followed by their resuspension in the same buffer. EPR samples in the presence of 0.5 mM PPBQ were prepared as described in refs *25* and *32*. EPR samples without PPBQ were prepared as follows. To synchronize all PSII in the $S_1Tyr_D^{\bullet}$ state, one preflash was given to the samples at room temperature, and the samples were kept in darkness at room temperature (16−18 °C) for 20−24 h. This long dark adaptation was shown to lead to the complete decay of Q_B^- (C. Fufezan and A. W. Rutherford, unpublished data). Then different numbers (from zero to three) of laser flashes (7 ns, 532 nm, 550 mJ) at 1 Hz were provided by an Nd:YAG laser (Spectra Physics), followed by rapid (1−2 s) freezing to 200 K (dry ice/ethanol) and storage at 77 K.

Before EPR measurements were made, all samples were degassed with argon at 200 K. Illumination at liquid helium temperature was carried out directly in the EPR cavity using a projector and a Perspex light guide. The light was provided by a 150 W projector lamp passing through a water filter with a path length of 3 cm and a narrow-band filter to obtain 680 ± 10 nm light. Under these conditions, there was no detectable heat effect on the samples during illumination as monitored by the effect of the illumination on stable signals (such as the Fe^{3+} signal at $g = 4.3$, the Cyt_{b559} signal, and the $Tyr_D^{\bullet}$ signal). Low-temperature continuous-wave EPR spectra and kinetics were recorded on a Bruker E300 spectrometer equipped with an Oxford-900 liquid helium cryostat and ITC-503 temperature controller (Oxford Instruments Ltd.). For the laser kinetic study, the laser flashes (7 ns, 532 nm, 550 mJ) were introduced directly into the EPR cavity. A Bruker ST4102 standard cavity was used for all the measurements. Spectrometer settings are given in the figure legends.

RESULTS

Figure 1A a shows the difference EPR spectrum, during illumination minus before illumination, recorded at 7 K for the zero-flash sample in isolated *T. elongatus* PSII, in which most centers were in the S_1 state. An EPR signal with a $g = 2.03$ peak was formed. No clear trough at high field side is distinguishable due to the absorption of $Tyr_D^{\bullet}$. This signal is similar to that reported in the S_1 state of PSII from spinach (see Figure 1B, spectrum a), which was assigned to $S_1Tyr_Z^{\bullet}$ (*24*−*27*). A similar signal was reported in a different thermophilic cyanobacterium when PSII was illuminated with IR light at liquid helium temperature when in the S_2 state, and this was also attributed to $S_1Tyr_Z^{\bullet}$ but formed by an IR-driven back-reaction from S_2 (*26*).

Spectrum b in Figure 1A shows the difference EPR spectrum, during illumination minus before illumination, recorded at 7 K for the three-flash sample, in which the dominant state is S_0 (ca. 60−70%). A wider EPR signal with a peak at low field ($g = 2.05$) and a trough at high field ($g = 1.95$) is clearly present, and the peak to trough width is ∼160 G. This signal is the same as that reported from the S_0 state in spinach (see Figure 1B, spectrum b), which was assigned to $S_0Tyr_Z^{\bullet}$ (*25*). Moreover, the shape at low and high field of this signal is symmetrical, which distinguishes it from the narrow $g = 2.03$ signal described above and a signal generated by near-IR light in the S_3 state (*33*, *34*; see also ref *35*) induced at low temperatures (below 77 K).

The inset in Figure 1A shows the induction and decay kinetics of these two signals from the zero- and three-flash samples, respectively. Both signals were induced rapidly by

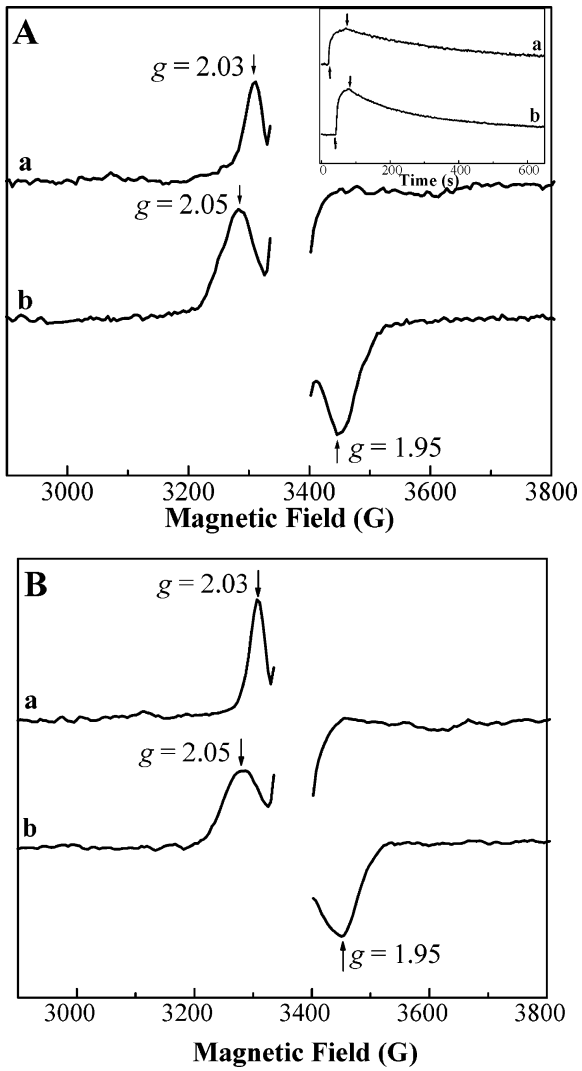

FIGURE 1: Difference EPR spectra (during illumination minus before illumination) recorded at 7 K from zero-flash (a) and three-flash (b) PSII samples from *T. elongatus* (A) and spinach (B) in the presence of 0.5 mM PPBQ. EPR conditions: temperature of 7 K, microwave frequency of 9.42 GHz, modulation frequency of 100 kHz, microwave power of 20 mW, modulation amplitude of 25 G, conversion time of 164 ms, time constant of 82 ms, sweep time of 168 s, receiver gain of 1.0×10^4, and four scans. The arrows indicate the position for the g values. The $g \approx 2.00$ region corresponding to the $Tyr_D^{\bullet}$ signal is omitted. In the inset, trace a shows the induction and decay kinetics of the narrow $g = 2.03$ signal from the zero-flash sample recorded by monitoring the EPR signal at 3310 G. Trace b is the induction and decay kinetic of the split signal from the three-flash sample recorded by monitoring the EPR signal at 3275 G. EPR conditions: conversion time of 1311 ms, time constant of 655 ms, sweep time of 1342 s, and receiver gain of 1.0×10^5. Other settings are the same as above. The arrows indicate when the lamp was turned on (↑) or off (↓).

visible light, and decayed on a minute time scale ($t_{1/2} \sim 5$ min) when the light was switched off. This behavior is also similar to that seen in plant PSII (*24*−*27*).

If these signals result from chlorophyll-based photochemistry within the reaction center, the oxidized donor-side species should be accompanied by a reduced acceptor-side species, most likely Q_A^-, with matching behavior. In these samples, the EPR signals arising from the $Q_A^-Fe^{2+}$ species are difficult to resolve. This is partially because the $Q_A^-Fe^{2+}$ $g \approx 1.9$ signal (*36*) present in the intact system is weak and the samples used for flash studies must be relatively dilute to allow saturation by the flash. The second difficulty, which is present for both samples but which is a particular problem for the three-flash sample, is that the light-induced signals around $g = 2$ overlap with the expected position of the $Q_A^-Fe^{2+}$ signal. A third problem is that the use of PPBQ as an external electron acceptor results in the oxidation of the non-heme iron (*37*, *38*). This certainly compromises the generation of the $Q_A^-Fe^{2+}$ state at low temperatures.

Figure 2 A shows a sample dark-adapted for 20 h without PPBQ. Under these conditions, despite the problems of spectral overlap described above, a weak $g \approx 1.9$ signal that can be attributed to $Q_A^-Fe^{2+}$ was detected following illumination (the $g = 1.87$ trough was used for the calculation, and is marked in Figure 2A). The $Q_A^-Fe^{2+}$ signal was formed and decayed with kinetics that matched the narrow split signal (Figure 2A, inset). This indicates that the $g = 2.03$ signal formed at low temperatures is the donor half of a semistable charge pair, in which the acceptor is Q_A^-. Given the weakness of the $Q_A^-Fe^{2+}$ signals and given early reports in which split signals have been suggested to have an acceptor side origin (*39*−*42*; also see the discussion in ref *28*), we looked for an additional way of confirming this result.

In PSII membrane preparations from plants, the function of the Q_B site is rarely conserved. However, in *T. elongatus*, Q_B is present in the core preparations (*43*). An $g = 1.66$ EPR signal (*44*) has been attributed to the $Q_A^-Fe^{2+}Q_B^-$ state (*45*, *46*). This signal is relatively strong, is present in the most intact material, and is shifted away from the $g = 2$ region. It may thus be used as a better probe of the Q_A^- state formed at low temperatures.

To form this signal, it is necessary to generate the Q_A^- state at temperatures sufficiently low to block electron transfer between the two quinones and in centers where the Q_B^- state is already present. In long dark-adapted PSII, Q_B^- is expected to be virtually absent; indeed, when samples were dark-adapted overnight, the $Q_A^-Fe^{2+}Q_B^-$ $g = 1.66$ signal was not detectable upon illumination at low temperatures (7 or 77 K). When the 77 K illuminated sample (containing $Q_A^-Fe^{2+}Q_B$) was thawed in the dark, incubated for 20 s, and then refrozen, we expected to have an increased concentration of $Q_A^-Fe^{2+}Q_B^-$. The subsequent illumination at low temperatures (7 or 77 K) resulted in very clear $g = 1.66$ signal arising from the $Q_A^-Fe^{2+}Q_B^-$ state (see Figure 2B). This low-temperature illumination/thaw-dark regime is an experimental procedure first introduced for identifying the origins of thermoluminescence bands in PSII (*47*).

Figure 2B shows that the $g = 1.66$ signal was generated by illumination at 7 K and decayed in the dark with kinetics that matched the $g = 2.03$ signal. This is further evidence that the $g = 2.03$ signal formed at 7 K in the S_1 state originates from the oxidized electron donor in a semistable charge pair involving Q_A^-.

For the split signal generated by 7 K illumination from the three-flash sample, attempts to study the $Q_A^-Fe^{2+}$ $g \approx 1.9$ signal were precluded by the complete overlap of the signals. We thus used the $g = 1.66$ signal from $Q_A^-Fe^{2+}Q_B^-$ instead. This required the generation of the S_0 state in the presence of Q_B^-. We found that omission of the artificial electron acceptor PPBQ from the flash series was sufficient for generation of this state. We observed that Q_B function

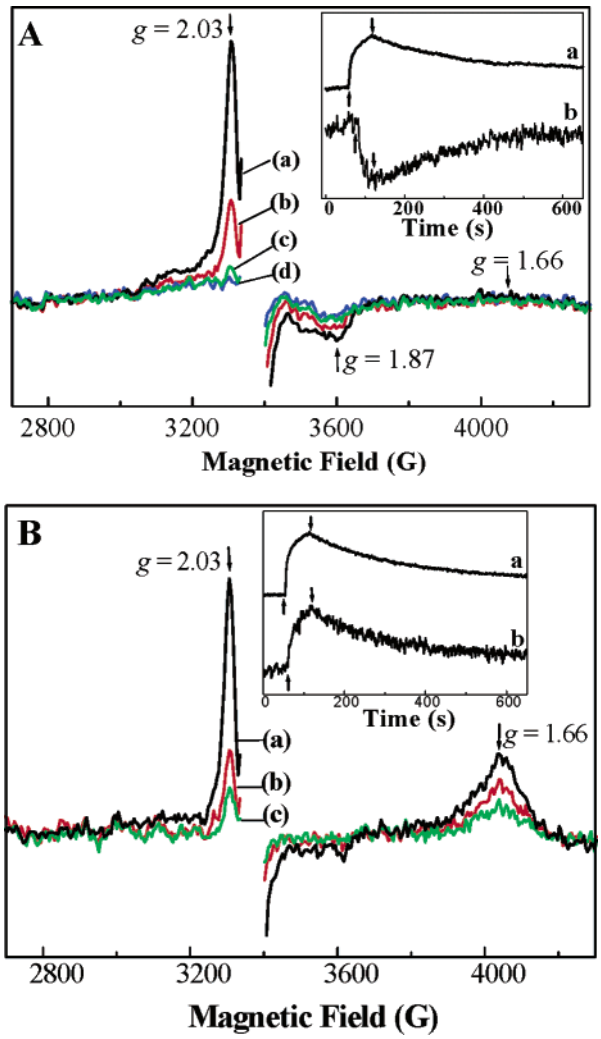

FIGURE 2: Time-dependent spectra after illumination of the long dark-adapted PSII core complex sample from *T. elongatus* without external quinone and without further treatment (A) and with 77 K illumination and the thaw-dark regime treatment (see the text) (B). The spectra in panel A are difference spectra with the spectra recorded at different times [(a) during illumination, (b) from 0 to 12 min after illumination, (c) from 12 to 24 min after illumination, and (d) from 24 to 36 min after illumination] minus the spectrum recorded before illumination at 7 K. Each is the accumulation of four scans. The inset in panel A shows the induction and decay kinetics of the $g = 2.03$ EPR signal [(a) recorded by monitoring the EPR signal at 3310 G] and the $g = 1.87$ signal [(b) recorded by monitoring the EPR signal at 3600 G] in the same sample. The spectra in panel B are difference spectra with the spectra recorded at different times [(a) during illumination, (b) from 0 to 24 min after illumination, and (c) from 24 to 48 min after illumination] minus the spectrum recorded before illumination at 7 K. The inset in panel B shows the induction and decay kinetics of the $g = 2.03$ EPR signal [(a) recorded by monitoring the EPR signal at 3310 G] and the $g = 1.66$ signal [(b) recorded by monitoring the EPR signal at 4045 G]. EPR conditions are the same as in Figure 1 except the receiver gain was 1.0×10^6 and 5.0×10^5 for trace b in the insets in panels A and B, respectively.

occurs in isolated *T. elongatus* PSII for at least three flashes. Figure 3 shows the difference spectra (during illumination minus before illumination at 7 K) obtained from the three-flash sample in the absence of an exogenous electron acceptor. The broad split signal and the $g = 1.66$ signal show matching kinetics for their formation upon illumination and their decay when the light is switched off (Figure 3, inset). These data clearly indicate that the broad split signal formed

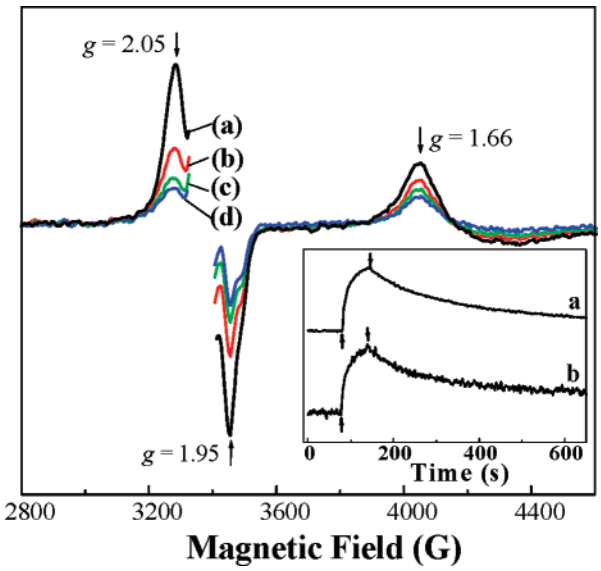

FIGURE 3: Time-dependent spectra after illumination of the three-flash PSII sample isolated from *T. elongatus* without external quinone after the long dark adaptation treatment. The difference spectra were obtained from the spectra recorded at different times [(a) during illumination, (b) from 0 to 12 min after illumination, (c) from 12 to 24 min after illumination, and (d) from 24 to 36 min after illumination] minus the spectrum recorded before illumination at 7 K. The $g \approx 2.00$ region corresponding to the $Tyr_D^{\bullet}$ absorption is omitted. EPR conditions are the same as in Figure 1. The inset shows the induction and decay kinetics of the $g = 2.05$ EPR signal [(a) recorded by monitoring the EPR signal at 3275 G] and the $g = 1.66$ signal [(b) recorded by monitoring the EPR signal at 4045 G] in the same sample. The EPR conditions were the same as in the inset in Figure 1A except the receiver gain in trace b is 5.0×10^5. The arrows indicate when the lamp was turned on (↑) or off (↓).

at 7 K in the S_0 state originates from the oxidized electron donor in a semistable charge pair involving Q_A^-.

Spectra a−d of Figure 3A are difference spectra recorded at different times after illumination minus the spectrum recorded before illumination. Some $Q_A^-Fe^{2+}Q_B^-$ ($g = 1.66$) signal remained present 36 min after illumination (spectrum d). This remained stable for several hours at 7 K. The stable $Q_A^-Fe^{2+}Q_B^-$ signal is attributed to centers in which electron donation from Cyt b_{559} or from Car/Chl_Z occurred (see below).

Having established the relationship between the 7 K light-induced $g = 2$ EPR signals and $Q_A^-Fe^{2+}$ or $Q_A^-Fe^{2+}$ Q_B^-, we should be able to estimate the number of centers in which the state is formed. Direct spin quantitation is not feasible for several reasons, including the lack of an appropriate reference signal, a lack of knowledge concerning the origin of the spin system responsible for the signals, and the overlap with the much larger $TyrD^{\bullet}$ signal. The most obvious alternative method is to compare the extent of the Q_A^- signal reversibly formed at 7 K with the maximum amount of the signal when Q_A^- is formed in all the centers. For the zero-flash sample, the difficulty is how to establish the maximum signal. It is usually assumed that strong illumination at 77 K will reduce Q_A^- to its full extent. We found that illumination under these conditions of a zero-flash dark-adapted sample did lead to an increase in the $Q_A^-Fe^{2+}$ signal. However, it was difficult to obtain an accurate measurement of this signal because of the appearance of a fraction of the Mn multiline signal that overlaps with the weak $g \approx 1.9$

signal from $Q_A^-Fe^{2+}$ (not shown). Furthermore, while the strong illumination at 77 K gradually removed the ability to generate the charge pair ($g = 2.03$ signal plus the $g \approx 1.9$ signal) at low temperatures, this did not go to completion (~25% of its ability to generate the charge pair remained) even after illumination for 40 min at 77 K. It is clear, therefore, that 77 K illumination did not generate the maximum quantity of Q_A^-.

For the zero-flash sample, we thus attempted to quantify the $Q_A^-Fe^{2+}$ signal based on a comparison of the semistable charge pair (measured as the reversible light-induced $Q_A^-Fe^{2+}$ signal at 7 K) with the stable charge pair (measured as the stable $Q_A^-Fe^{2+}$ signal formed at 7 K). First, however, the number of centers giving rise to the stable charge pair under these conditions needed to be established.

The stable charge pair is formed at low quantum yield via donation from Car to $P_{680}^{+\bullet}$ (*48*, *49*). When Cyt b_{559} is reduced prior to illumination, it donates to the Car cation (*49*). When Cyt b_{559} is oxidized prior to illumination, the cation radical remains on the Car or moves to the Chl_Z, a process that is temperature- and species-dependent (*48*, *50*).

Thus, we estimated the number of centers in which the Cyt is photooxidized at 7 K by comparing the light-induced EPR signal from the oxidized heme with its EPR signal when fully oxidized. Figure 4A shows the spectra of the g_Z region of the low-spin ferric hemes. There are two cytochromes present in the PSII sample from *T. elongatus*, Cyt b_{559} and Cyt c_{550}, (*1*−*3*, *51*). Cyt c_{550} has a potential of −80 mV (*52*); thus, it remains oxidized under these conditions. The Cyt b_{559} is expected to be in its reduced form prior to illumination in a variable fraction of centers depending on the samples' pretreatment, and this can undergo oxidation when illuminated at low temperatures (*53*, *54*). The oxidized states of the two cytochromes have similar EPR spectra (*52*, *55*).

In our dark sample, we expect to have a contribution from all of the Cyt c_{550} heme plus any low-potential form of Cyt b_{559} that happens to be present in the sample. Our washing treatment to remove the glycerol (see Materials and Methods) is likely to have led to an increase in the level of the low-potential form.

Illumination at 7 K produced a small stable increase in the magnitude of the g_Z peak of the oxidized cytochrome (Figure 4A, spectra a and b), indicating the additional oxidation of a small fraction of Cyt b_{559}. The maximum absorption of the oxidized cytochrome in the sample can be obtained by treatment with 2 mM K_2IrCl_6 (*53*, *54*), as shown in spectrum c of Figure 5A. If we assume as a first approximation that the two hemes have comparable amplitudes in their g_Z signals, then we can make an approximate quantification based on the idea that the fully oxidized sample is equal to two spins (200%), and thus, the Cyt b_{559} induced by visible light at 7 K can be calculated to be approximately 11%.

We also estimated the number of centers in which either the Car or Chl_Z cation radical is formed by comparing the $g \approx 2.003$ signal with the signal from the stable $Tyr_D^{\bullet}$. Figure 4B shows the change in the radical spectra before (spectrum a) and after illumination (spectrum b), and the difference spectrum (spectrum c). The amount of the radical formed can be determined by comparing the double integration of the $Tyr_D^{\bullet}$ absorption (spectrum a) and the signal induced by

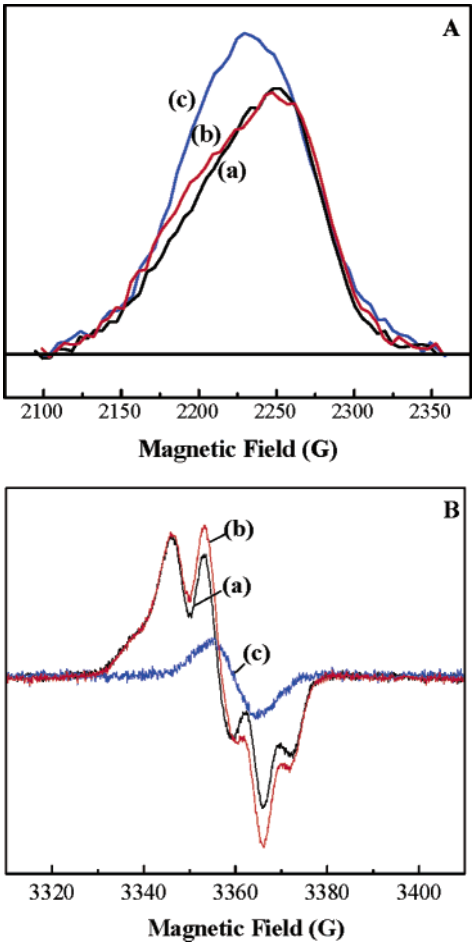

FIGURE 4: (A) g_Z EPR spectra from the low-spin cytochromes. Spectrum a was recorded before illumination; spectrum b was recorded 30 min after illumination at 7 K, and spectrum c was recorded after treatment with 2 mM K_2IrCl_6 and corresponds to the fully oxidized form of both cytochromes. EPR conditions: temperature of 15 K and microwave power of 5 mW. Other settings are the same as in Figure 1A. (B) EPR spectra for $Tyr_D^{\bullet}$ and the radical region. Spectrum a was recorded before illumination; spectrum b was recorded 30 min after illumination, and spectrum c is the difference spectrum between spectrum b and spectrum a. EPR conditions: temperature of 15 K, microwave power of 5 μW, modulation amplitude of 2.8 G, conversion time of 82 ms, time constant of 41 ms, and sweep time of 82 s. Other settings are the same as in Figure 1A.

light (spectrum c). In this experiment, we estimate that the oxidation of Car/Chl_Z occurs in approximately 16% reaction centers.

Therefore, the total amount of the reaction centers corresponding to the oxidation of Cyt b_{559} and Car/Chl_Z is approximately 27%. The proportion of centers involved in formation of the semistable charge pair can now be estimated by comparing the amplitude of the $Q_A^-Fe^{2+}$ signal ($g = 1.87$) formed at 7 K with that from the stable charge pair. This gives us approximately 40% of centers.

The same approaches can be taken on the basis of the $g = 1.66$ signal from $Q_A^-Fe^{2+}Q_B^-$ in samples treated as described in the legend of Figure 2B. The number of centers in which electron donation from the side-path donors occurs is estimated by this method to be approximately 29%. The estimated yield from the S_1 sample was lower than that obtained by using the $Q_A^-Fe^{2+}$ signal ($g = 1.87$) in the untreated zero-flash sample described above. The main

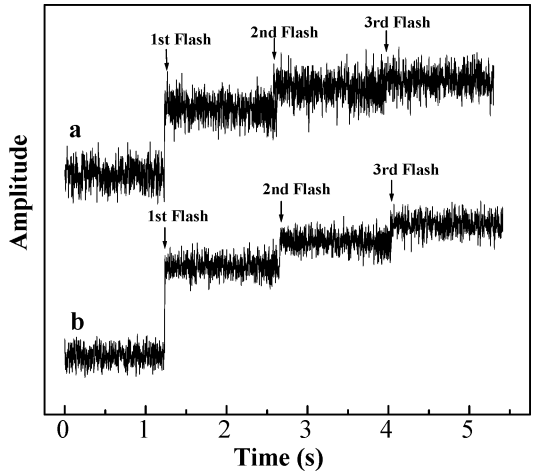

FIGURE 5: Time-resolved EPR measurements of the laser flash induction of the split signal from three-flash (trace a) and zero-flash (trace b) spinach PSII samples at 7 K. Trace a was recorded by monitoring the broad split EPR signal at 3275 G ($g = 2.05$) from the three-flash sample. Trace b was recorded by monitoring the EPR signal at 3310 G ($g = 2.03$) from the zero-flash sample. EPR conditions: temperature of 7 K, microwave frequency of 9.42 GHz, modulation frequency of 100 kHz, microwave power of 20 mW, modulation amplitude of 25 G, conversion time of 1.28 ms, time constant of 1.28 ms, and receiver gain of 1.0×10^5.

reason for this difference is that Q_A^- is reduced in only ~75% of the centers after visible light illumination for 40 min at 77 K, and therefore, the fraction of Q_B^- formed after subsequent dark adaptation at 0 °C is at best 75%. When this is taken into consideration, on the basis of the $g = 1.66$ signal the estimate of the number of centers involved in the formation of the reversible charge pair at 7 K is approximately 39%, almost the same as that obtained by monitoring the $g = 1.87$ $Q_A^-Fe^{2+}$ signal (described above).

For the three-flash sample, using the same methods and on the basis of the $g = 1.66$ signal from $Q_A^-Fe^{2+}Q_B^-$, the percentage of centers involved in the semistable charge pair at 7 K was found to be approximately 32%. When the misses involved in the formation of the S_0 state upon three flashes are taken into account, this is equivalent to ~46−53% of the centers in the S_0 state.

For the S_0 state, we found that a period of strong illumination at 77 K resulted in the complete loss of the ability to form the semistable charge pair at 7 K. Under these conditions, we could take the extent of the $g = 1.66$ signal as a true signal maximum. The size of the $g = 1.66$ signal involved in the reversible charge pair was 41% of this signal. When the predicted S state distribution after three flashes is taken into account, this is equivalent to 58−68% of the centers in the S_0 state.

Given that the EPR signals occurring in *T. elongatus* are similar to those formed under the same conditions in plant PSII, and that they arise from the same chemical states, in principle it should be possible to estimate the yield of these states in plant PSII based on comparing the signal amplitudes (see Figure 1). By normalizing to the extent of the EPR signal arising from $Tyr_D^{\bullet}$, and using identical measuring conditions, we found the yields of the signals in plant PSII to be 68 and 50% in S_1 and S_0, respectively. The value for S_0 is similar to that in *T. elongatus*, while the value for S_1 is larger in plant PSII. We consider the value for the S_1 state in plant PSII to be an overestimate due to the influence of trace quantities of glycerol on the $g = 2.03$ signal in the *T. elongatus* sample, since glycerol greatly diminishes the amplitude of this signal (data not shown).

Figure 5a shows the S_0 split signal is induced by laser flashes at 7 K in a spinach PSII sample that had been given three flashes at room temperature prior to freezing. A prompt rise (within our instrument response) of the split signal was observed upon a single laser flash. The amplitude of this signal (trace a) was ~75% of that obtained by continuous illumination of this sample. In contrast, no detectable increases in the oxidized Cyt b_{559} and/or Car/Chl_Z radical EPR signals were observed after the first laser flash (data not shown). The second laser flash (1 s after the first flash) induced ~20% of the broad split signal, and a very small increase in the split signal was observed after further flashes. Figure 5b shows similar results for the formation of the $g = 2.03$ signal in the sample in the S_1 state.

DISCUSSION

Two metalloradical EPR signals at around $g = 2$ are induced by visible light at liquid helium temperature in the PSII core complexes from *T. elongatus*. These signals are associated with the S_0 and S_1 states; they are stable for a few minutes after illumination at low temperatures, and they are similar to signals reported in PSII-enriched membranes from plants (*24*−*27*). The induction and decay of both signals correspond to the appearance and disappearance of Q_A^- signals (both the $Q_A^-Fe^{2+}$ $g \approx 1.9$ signal and the $Q_A^-Fe^{2+}Q_B^-$ $g = 1.66$ signal were monitored), indicating that they arise from light-induced charge separation followed by charge recombination in darkness. This result fits with earlier proposals for the origin of these signals in plant PSII, but the clear relationship with the electron acceptor signal puts these assignments on a much more solid basis.

By using the $Q_A^-Fe^{2+}$ and $Q_A^-Fe^{2+}Q_B^-$ EPR signals and signals from Cyt b_{559} and the Car/Chl_Z radicals, the yields of the two metalloradical EPR signals were estimated. The semistable charge separation was estimated to occur in approximately 50 and 40% of the centers in the S_0 and S_1 states, respectively. Earlier estimates (*24*, *25*) were comparable to those given here; however, the agreement is probably fortuitous since both approaches that were used earlier seem unreliable. We further observed here that a single laser flash could induce more than 75% of the maximum amplitude of the split signals at 7 K.

While we have not provided direct evidence for identifying the metalloradical signals as arising from Tyr_Z, we consider that the observations presented here are consistent with this interpretation. The existence of the signals in *T. elongatus*, their high quantum yields of formation, their occurrence in a significant fraction centers, and the demonstration that they are formed as one-half of a semistable charge pair involving Q_A^- are all good indications that they arise from an electron donor that is involved in rapid electron donation to P_{680}^+, stabilizing the $P_{680}^+Q_A^-$ charge pair, which is expected to have a lifetime of a few milliseconds under these conditions. It seems reasonable that electron donation from Tyr_Z might be expected to occur in this time range or faster at 7 K since we have observed that Tyr_D is able to donate to $P_{680}^{+\bullet}$ in the tens of microseconds time range at similar temperatures (P. Faller, K. Brettel, and A. W. Rutherford unpublished results).

Thus, on the basis of this work and previous reports (*24*−*27*), we conclude that it seems likely that a high yield of Tyr_Z oxidation can be achieved by illumination with visible light at liquid helium temperature, and $S_0Tyr_Z^{\bullet}$ and $S_1Tyr_Z^{\bullet}$ signals are formed in the S_0 and S_1 states, respectively, in active PSII. These results change the view of what occurs in low-temperature photochemistry in PSII. It has long been held that electron donation from the Tyr_Z shuts off as the temperature is lowered, being replaced by $P_{680}^{+}Q_A^{-}$ formation and decay (*16*, *18*, *56*, *57*). There is good evidence that this occurs (*16*, *18*, *56*) and that P_{680}^{+} can be reduced at a low quantum yield by Car forming the $Car^{+}Q_A^{-}$ charge pair (*48*). This charge pair can be reduced by Cyt b_{559} or Chl_Z, forming the relatively stable Cyt $b_{559ox}Q_A^{-}$ or $Chl_Z^{+}Q_A^{-}$ charge pair (*48*, *50*). This picture must be modified on the basis of the work presented here (and see also refs *24*−*27*) that indicates that in the active enzyme [but not the Mn-depleted enzyme (*22*)], for nearly half the centers, this is not the case. In these centers, high-quantum yield electron donation to P_{680}^{+} appears to be possible, giving rise to a relatively stable state at low temperatures, which can be attributed to the $Tyr_Z^{\bullet}Q_A^{-}$ state. This state recombines on the minutes time scale at 7 K and presumably faster at 77 K.

In more than half of the centers, the traditional picture holds, yet it is assumed that the sample is relatively homogeneous in terms of function at room temperature. However, kinetic studies of the enzyme at room temperature have shown that the kinetics of electron donation are multiphasic with the most rapid electron donation occurring in less than half of the centers and slower kinetics occurring in the other centers (see refs *58*−*61*). This presumably represents an equilibrium that is present prior to excitation. Freezing of the sample could lock in this heterogeneity and thus give rise to the two types of centers observed here.

Long illumination at 77 K does lead to a decrease in the number of centers able to form the state attributed to $S_1Tyr_Z^{\bullet}Q_A^{-}$ and $S_0Tyr_Z^{\bullet}Q_A^{-}$. We assume that the low-quantum yield electron donation from Car (and thence Cyt b_{559} or Chl_Z) can, in time, compete with the electron donation from Tyr_Z and the $P_{680}^{+}Q_A^{-}$ recombination, and as the lowest-energy state, this pathway will eventually produce the final stable charge pair.

The frozen-in heterogeneity should be present in optical studies. So far, no reports of this kind have appeared. This could be due to an influence of glycerol (generally used in the optical studies) blocking the fast kinetics at low temperatures, and indeed, here we found that glycerol eliminates the formation of the $g = 2.03$ signal in the S_1 state [note, however, that in plant PSII glycerol appears to change the stability of the $g = 2.03$ signal (*24*)]. Alternatively, a fraction of the centers undergoing photochemistry with a high quantum yield producing a relatively stable state could have been missed in previous studies. We are currently looking into these possibilities.

The nature of the reaction occurring at low temperatures has been discussed previously (*24*, *25*), but as for Tyr_D oxidation at low temperatures (*23*), we consider two models: (a) one in which tyrosine is deprotonated prior to oxidation and thus the low-temperature reaction is a pure electron transfer reaction and (b) one in which a proton-coupled electron transfer occurs with the deprotonation occurring across an appropriate hydrogen bond to D1-His190. Further spectroscopic studies are required to distinguish between these options.

ACKNOWLEDGMENT

We thank M. Sugiura for providing the His-tagged strain of the cyanobacterium and M. Sugiura and D. Kirilovsky for their contributions in developing the conditions for the culture of the cyanobacteria and the isolation of PSII. C.Z. thanks S. Styring for helpful discussion.

REFERENCES

1. Zouni, A., Witt, H. T., Kern, J., Fromme, P., Krauss, N., Saenger, W., and Orth, P. (2001) Crystal structure of photosystem II from *Synechococcus elongatus* at 3.8 Å resolution, *Nature 409*, 739−743.
2. Kamiya, N., and Shen, J. R. (2003) Crystal structure of oxygen-evolving photosystem II from *Thermosynechococcus vulcanus* at 3.7-Å resolution, *Proc. Natl. Acad. Sci. U.S.A. 100*, 98−103.
3. Ferreira, K. N., Iverson, T. M., Maghlaoui, K., Barber, J., and Iwata, S. (2004) Architecture of the photosynthetic oxygen-evolving center, *Science 303*, 1831−1838.
4. Britt, R. D. (1996) Oxygen evolution, in *Oxygenic Photosynthesis: The Light Reactions* (Ort, D. R., and Yocum, C. F., Eds.) pp 137−164, Kluwer Academic Publishers, Dordrecht, The Netherlands.
5. Diner, B. A., and Babcock, G. T. (1996) Structure, dynamics, and energy conversion efficiency in photosystem II, in *Oxygenic Photosynthesis: The Light Reactions* (Ort, D. R., and Yocum, C. F., Eds.) pp 213−247, Kluwer Academic Publishers, Dordrecht, The Netherlands.
6. Debus, R. J. (1992) The manganese and calcium ions of photosynthetic oxygen evolution, *Biochim. Biophys. Acta 1102*, 269−352.
7. Diner, B. A., and Rappaport, F. (2002) Structure, dynamics, and energetics of the primary photochemistry of photosystem II of oxygenic photosynthesis, *Annu. Rev. Plant Biol. 53*, 551−580.
8. Goussias, C., Boussac, A., and Rutherford, A. W. (2002) Photosystem II and photosynthetic oxidation of water: an overview, *Philos. Trans. R. Soc. London, Ser. B 357*, 1369−1381.
9. Mino, H., and Kawamori, A. (1994) Microenvironments of tyrosine D^{+} and tyrosine Z^{+} in photosystem II studied by proton matrix ENDOR, *Biochim. Biophys. Acta 1185*, 213−222.
10. Tommos, C., Tang, X. S., Warncke, K., Hoganson, C. W., Styring, S., McCracken, J., Diner, B. A., and Babcock, G. T. (1995) Spin-density distribution, donformation, and hydrogen bonding of the redox-active tyrosine Y_Z in photosystem II from multiple-electron magnetic-resonance spectroscopies: implications for photosynthetic oxygen evolution, *J. Am. Chem. Soc. 117*, 10325−10335.
11. Tang, X. S., Zheng, M., Chisholm, D. A., Dismukes, G. C., and Diner, B. A. (1996) Investigation of the differences in the local protein environments surrounding tyrosine radicals $Y_Z^{\bullet}$ and $Y_D^{\bullet}$ in photosystem II using wild-type and the D2-Tyr160Phe mutant of *Synechocystis* 6803, *Biochemistry 35*, 1475−1484.
12. Boussac, A., Zimmermann, J. L., and Rutherford, A. W. (1989) EPR signals from modified charge accumulation states of the oxygen-evolving enzyme in calcium-deficient photosystem II, *Biochemistry 28*, 8984−8989.
13. Gilchrist, M. L., Jr., Ball, J. A., Randall, D. W., and Britt, R. D. (1995) Proximity of the maganese cluster of photosystem II to the redox-active tyrosine Y_Z, *Proc. Natl. Acad. Sci. U.S.A. 92*, 9545−9549.
14. Debus, R. J. (2001) Amino acid residues that modulate the properties of tyrosine Y_Z and the manganese cluster in the water oxidizing complex of photosystem II, *Biochim. Biophys. Acta 1503*, 164−186.
15. Diner, B. A. (2001) Amino acid residues involved in the coordination and assembly of the manganese cluster of photosystem II. Proton-coupled electron transport of the redox-active tyrosines and its relationship to water oxidation, *Biochim. Biophys. Acta 1503*, 147−163.
16. Mathis, P., and Vermeglio, A. (1975) Chlorophyll radical cation in photosystem II of chloroplasts. Millisecond decay at low temperature, *Biochim. Biophys. Acta 396*, 371−381.

17. Babcock, G. T., Barry, B. A., Debus, R. J., Hoganson, C. W., Atamian, M., McIntosh, L., Sithole, I., and Yocum, C. F. (1989) Water oxidation in photosystem II: from radical chemistry to multielectron chemistry, *Biochemistry 28*, 9557−9565.
18. Kühne, H., and Brudvig, G. W. (2002) Proton-coupled electron-transfer involving tyrosine Z in photosystem II, *J. Phys. Chem. B 106*, 8189−8196.
19. Styring, S., and Rutherford, A. W. (1988) Deactivation kinetics and temperature dependence of the S-state transitions in the oxygen-evolving system of photosystem II measured by EPR spectroscopy, *Biochim. Biophys. Acta 933*, 378−387.
20. Koike, H., and Inoue, Y. (1987) Temperature dependence of the S-state transition in a thermophilic cyanobacterium measured by thermoluminescence, in *Progress in Photosynthesis Research* (Biggins, J., Ed.) Vol. 1, pp 645−648, Martinus Nijhoff, Dordrecht, The Netherlands.
21. Brudvig, G. W., Casey, J. L., and Sauer, K. (1983) The effect of temperature on the formation and decay of the multilane EPR signal species associated with photosynthetic oxygen evolution, *Biochim. Biophys. Acta 723*, 366−371.
22. Faller, P., Rutherford, A. W., and Debus, R. J. (2002) Tyrosine D oxidation at cryogenic temperature in photosystem II, *Biochemistry 41*, 12914−12920.
23. Faller, P., Goussias, C., Rutherford, A. W., and Un, S. (2003) Resolving intermediates in biological proton-coupled electron transfer: A tyrosyl radical prior to proton movement, *Proc. Natl. Acad. Sci. U.S.A. 100*, 8732−8735.
24. Nugent, J. H. A., Muhiuddin, I. P., and Evans, M. C. W. (2002) Electron transfer from the water oxidizing complex at cryogenic temperatures: the S_1 to S_2 step, *Biochemistry 41*, 4117−4126.
25. Zhang, C., and Styring, S. (2003) Formation of split electron paramagnetic resonance signals in photosystem II suggests that tyrosine$_Z$ can be photooxidized at 5 K in the S_0 and S_1 states of the oxygen-evolving complex, *Biochemistry 42*, 8066−8076.
26. Koulougliotis, D., Shen, J. R., Ioannidis, N., and Petrouleas, V. (2003) Near-IR irradiation of the S_2 state of the water oxidizing complex of photosystem II at liquid helium temperatures produces the metalloradical intermediate attributed to $S_1Y_Z^{\bullet}$, *Biochemistry 42*, 3045−3053.
27. Nugent, J. H. A., Muhiuddin, I. P., and Evans, M. C. W. (2001) Studies on the interaction between tyrosine Y_Z and the Mn complex, in *PS2001 Proceeding of 12th International Congress on Photosynthesis*, Brisbane, Australia, Aug 18−23, 2001, S10-012.
28. Nugent, J. H. A., Muhiuddin, I. P., and Evans, M. C. W. (2003) Effect of hydroxylamine on photosystem II: reinvestigation of electron paramagnetic resonance characteristics reveals possible S state intermediates, *Biochemistry 42*, 5500−5507.
29. Berthold, D. A., Babcock, G. T., and Yocum, C. F. (1981) A highly resolved, oxygen-evolving photosystem II preparation from spinach thylakoid membranes, *FEBS Lett. 134*, 231−234.
30. Campbell, K. A., Gregor, W., Pham, D. P., Peloquin, J. M., Debus, R. J., and Britt, R. D. (1998) The 23 and 17 kDa extrinsic proteins of photosystem II modulate the magnetic properties of the S_1-state manganese cluster, *Biochemistry 37*, 5039−5045.
31. Sugiura, M., and Inoue, Y. (1999) Highly purified thermo-stable oxygen-evolving photosystem II core complex from the thermophilic cyanobacterium *Synechococcus elongatus* having His-tagged CP43, *Plant Cell Physiol. 40*, 1219−1231.
32. Styring, S., and Rutherford, A. W. (1988) The microwave power saturation of SII_{slow} varies with the redox state of the oxygen-evolving complex in photosystem II, *Biochemistry 27*, 4915−4923.
33. Ioannidis, N., and Petrouleas, V. (2000) Electron paramagnetic resonance signals from the S_3 state of the oxygen-evolving complex. A broadened radical signal induced by low-temperature near-infrared light illumination, *Biochemistry 39*, 5246−5254.
34. Boussac, A., Sugiura, M., Inoue, Y., and Rutherford, A. W. (2000) EPR study of the oxygen evolving complex in His-tagged photosystem II from the cyanobacterium *Synechococcus elongatus*, *Biochemistry 39*, 13788−13799.
35. Nugent, J. H. A., Turconi, S., and Evans, M. C. W. (1997) EPR investigation of water oxidizing photosystem II: Detection of new EPR signals at cryogenic temperatures, *Biochemistry 36*, 7086−7096.
36. Rutherford, A. W., and Zimmermann, J. L. (1984) A new EPR signal attributed to the primary plastosemiquinone acceptor in photosystem II, *Biochim. Biophys. Acta 767*, 168−175.
37. Zimmermann, J. L., and Rutherford, A. W. (1986) Photoreduction-induced oxidation of Fe^{2+} in the electron-acceptor complex of photosystem II, *Biochim. Biophys. Acta 851*, 416−423.
38. Petrouleas, V., and Diner, B. A. (1987) Light-induced oxidation of the acceptor-side Fe(II) of photosystem II by exogenous quinines acting through the Q_B binding site. I. Quinone, kinetics and pH-dependence, *Biochim. Biophys. Acta 893*, 126−137.
39. Vermaas, W. F. J., and Rutherford, A. W. (1984) EPR measurements on the effects of bicarbonate and triazine resistance on the acceptor side of photosystem II, *FEBS Lett. 175*, 243−247.
40. Beck, W. F., and Brudvig, G. W. (1987) Reactions of hydroxylamine with the electron-donor side of photosystem II, *Biochemistry 26*, 8285−8295.
41. Sivaraja, M., and Dismukes, G. C. (1988) Binding of hydroxylamine to the water-oxidizing complex and the ferroquinone electron acceptor of spinach photosystem II, *Biochemistry 27*, 3467−3475.
42. Sivaraja, M., and Dismukes, G. C. (1988) Inhibition of electron transport in photosystem II by hydroxylamine: further evidence for two binding sites, *Biochemistry 27*, 6297−6306.
43. Kuhl, H., Krieger, A., Seidler, A., Boussac, A., Rutherford, A. W., and Rögner, M. (1998) Characterisation and functional studies on a new photosystem 2 preparation from the thermophilic cyanobacterium *Synechococcus elongates*, in *Photosynthesis: Mechanisms and Effects* (Garab, G., Ed.) Vol. II, pp 1001−1004, Kluwer Academic Publishers, Dordrecht, The Netherlands.
44. McDermott, A. E., Yachandra, V. K., Guiles, R. D., Cole, J. L., Dexheimer, S. L., Britt, R. D., Sauer, K., and Klein, M. P. (1988) Characterization of the manganese oxygen-evolving complex and the iron-quinone acceptor complex in photosystem II from a thermophilic cyanobacterium by electron paramagnetic resonance and X-ray absorption spectroscopy, *Biochemistry 27*, 4021−4031.
45. Hallahan, B. J., Ruffle, S. V., Bowden, S. J., and Nugent, J. H. A. (1991) Identification and characterisation of EPR signals involving Q_B semiqinone in plant photosystem II, *Biochim. Biophys. Acta 1059*, 181−188.
46. Corrie, A. R., Nugent, J. H. A., and Evans, M. C. W. (1991) Identification of EPR signals from the states $Q_A^{\bullet-}Q_B^{\bullet-}$ and $Q_B^{\bullet-}$ in photosystem II from *Phormidium laminosum*, *Biochim. Biophys. Acta 1057*, 384−390.
47. Rutherford, A. W., Crofts, A. R., and Inoue, Y. (1982) Thermoluminescence as a probe of photosystem II photochemistry: the origin of the flash-induced glow peaks, *Biochim. Biophys. Acta 682*, 457−465.
48. Hanley, J., Deligiannakis, Y., Pascal, A., Faller, P., and Rutherford, A. W. (1999) Carotenoid oxidation in photosystem II, *Biochemistry 38*, 8189−8195.
49. Faller, P., Pascal, A., and Rutherford, A. W. (2001) β-Carotene Redox Reactions in Photosystem II: Electron Transfer Pathway, *Biochemistry 40*, 6431−6440.
50. Tracewell, C. A., Cua, A., Stewart, D. H., Bocian, D. F., and Brudvig, G. W. (2001) Characterization of Carotenoid and Chlorophyll Photooxidation in Photosystem II, *Biochemistry 40*, 193−203.
51. Shen, J. R., and Inoue, Y. (1993) Binding and functional properties of two new extrinsic components, cytochrome c-550 and a 12-kDa protein, in cyanobacterial photosystem II, *Biochemistry 32*, 1825−1832.
52. Roncel, M., Boussac, A., Zurita, J. L., Bottin, H., Sugiura, M., Kirilovsky, D., and Ortega, J. M. (2003) Redox properties of the photosystem II cytochromes b559 and c550 in the cyanobacterium *Thermosynechococcus elongatus*, *J. Biol. Inorg. Chem. 8*, 206−216.
53. Stewart, D. H., and Brudvig, G. W. (1998) Cytochrome b559 of photosystem II, *Biochim. Biophys. Acta 1367*, 63−87.
54. Buser, C. A., Diner, B. A., and Brudvig, G. W. (1992) Reevaluation of the stoichiometry of cytochrome b559 in photosystem II and thylakoid membranes, *Biochemistry 31*, 11441−11448.
55. Kerfeld, C. A., Sawaya, M. R., Bottin, H., Tran, K. T., Sugiura, M., Cascio, D., Desbois, A., Yeates, T. O., Kirilovsky, D., and Boussac, A. (2003) Structural and EPR characterizaton of the soluble form of cytochrome *c*-550 and of the *psbv2* gene product from the cyanobacterium *Thermosynechococcus elongates*, *Plant Cell Physiol. 44*, 697−706.

56. Hillmann, B., and Schlodder, E. (1995) Electron transfer reactions in photosystem II core complexes from *Synechcoccus* at low temperature: difference spectrum of $P_{680}^{+}Q_A^{-}/P_{680}Q_A$ at 77 K, *Biochim. Biophys. Acta 1231*, 76−88.
57. Noguchi, T., Mitsuka, T., and Inoue, Y. (1994) Fourier-transform infrared spectrum of the radical cation of β-carotene photoinduced in photosystem II, *FEBS Lett. 356*, 179−182.
58. Brettel, K., Schlodder, E., and Witt, H. T. (1984) Nanosecond reduction kinetics of photooxidized chlorophyll-a II (P-680) in single flashes as a probe for the electron pathway, H^{+}-release and charge accumulation in the O_2-evolving complex, *Biochim. Biophys. Acta 766*, 403−415.
59. Jeans, C., Schilstra, M. J., and Klug, D. R. (2002) The temperature dependence of P_{680}^{+} reduction in oxygen-evolving photosystem II, *Biochemistry 41*, 5015−5023.
60. Eckert, H. J., and Renger, G. (1988) Temperature dependence of P_{680}^{+} reduction in O_2-evolving PSII membrane fragments at different redox states S_i of the water oxidation system, *FEBS Lett. 236*, 425−431.
61. Renger, G. (2001) Photosynthetic water oxidation to molecular oxygen: apparatus and mechanism, *Biochim. Biophys. Acta, 1503*, 210−228.

BI048631J